

# Azimuthal anisotropy of $K_S^0$ and $\Lambda$ production at mid-rapidity from Au+Au collisions at $\sqrt{s_{NN}} = 130$ GeV

Paul Sorensen for the STAR Collaboration

University of California, Los Angeles, California 90095

**Abstract.** We report STAR results on the azimuthal anisotropy parameter  $v_2$  for strange particles  $K_S^0$  and  $\Lambda$  at mid-rapidity in Au+Au collisions at  $\sqrt{s_{NN}} = 130$  GeV at RHIC. The value of  $v_2$  as a function of transverse momentum  $p_t$  and collision centrality is presented for both particles and compared with model calculations. A strong  $p_t$  dependence in  $v_2$  is observed up to  $p_t \sim 2.0$  GeV/c where  $v_2$  begins to saturate.

## INTRODUCTION

Measurements of azimuthal anisotropies in the transverse momentum distributions of particles probe early stages of ultra-relativistic heavy-ion collisions [1, 2, 3]. After an initial geometric anisotropy is established in an off-center or non-central collision, rescattering in the overlapping region of the colliding nuclei amongst collision participants transfers the spatial anisotropy into an anisotropy in momentum space. The extent of the transformation depends on the initial conditions and the dynamical evolution of the collision. As a result, anisotropy measurements for nucleus-nucleus collisions at RHIC energies may increase our understanding of the processes governing the evolution of the collision system and in particular, may provide information about an early partonic stage in the evolution of the system [1, 4, 5, 6, 7, 8].

For the purpose of studying azimuthal anisotropies it is advantageous to write the triple differential distribution of particles in the form of a Fourier series

$$E \frac{d^3N}{d^3p} = \frac{1}{2\pi} \frac{d^2N}{p_t dp_t dy} \left( 1 + \sum_{n=1}^{\infty} 2v_n \cos(n\phi) \right), \quad (1)$$

where  $p_t$  is the transverse momentum of the particle,  $y$  is its rapidity and  $\phi$  denotes its azimuthal angle of emission with respect to the true reaction plane angle<sup>1</sup> [9, 10]. The harmonic coefficients  $v_n$  are anisotropy parameters and the second coefficient  $v_2$  is called the *elliptic flow* parameter. Recent experimental results from RHIC [11, 12, 13, 14] include measurements of  $v_2$  as a function of collision centrality and  $p_t$  for charged

---

<sup>1</sup> The reaction plane is the plane defined by the beam line and the line connecting the centers of the colliding nuclei.

particles up to a  $p_t$  of about 2.0 GeV/c, and for identified  $\pi^\pm$ ,  $K^\pm$  and  $p(\bar{p})$  up to a  $p_t$  of about 0.8 GeV/c.

We report on the first measurement of the azimuthal anisotropy parameter  $v_2$ , as a function of  $p_t$  and collision centrality, for the strange particles  $K_S^0$  and  $\Lambda$  from minimum bias Au + Au collisions at  $\sqrt{s_{NN}} = 130$  GeV. Our measurements of  $v_2$  for identified particles using the Solenoidal Tracker At RHIC (STAR) are the first to extend beyond the  $p_t$  range where particles are identified by their specific energy loss (dE/dx) in the gas of the Time Projection Chamber (TPC), and up to  $p_t \sim 3.0$  GeV/c. Previously  $v_2$  in this higher  $p_t$  range had only been measured for unidentified charged particles [15].

## ANALYSIS

The STAR detector [16], due to its azimuthal symmetry and large acceptance, is ideally suited for measuring elliptic flow. For collisions in its center, the STAR TPC measures the tracks of charged particles in the pseudo-rapidity range  $|\eta| < 1.8$  with  $2\pi$  azimuthal coverage. A scintillator barrel, the Central Trigger Barrel (CTB), surrounding the TPC that measures the charged particle multiplicity within  $|\eta| < 1$  was used for a central trigger. Two Zero-Degree Calorimeters [17] at both ends of the TPC in coincidence provided a minimum bias trigger.

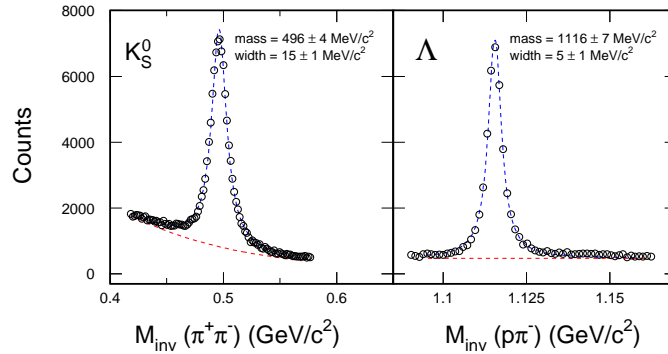


**FIGURE 1.** Invariant mass distributions for  $\pi^+\pi^-$  showing an enhancement at the  $K_S^0$  mass (left panel) and  $p\pi^-$  ( $\bar{p}\pi^+$ ) showing an enhancement at the  $\Lambda$  ( $\bar{\Lambda}$ ) mass (right panel). Fitting results are shown as dashed lines in the figure.

The masses and kinematic properties of both  $K_S^0 \rightarrow \pi^+ + \pi^-$  and  $\Lambda(\bar{\Lambda}) \rightarrow p + \pi^-$  ( $\bar{p} + \pi^+$ ), are reconstructed via their decay topologies in the TPC [18, 19, 20]. Figure 1 shows the invariant mass distributions for a  $\pi^+\pi^-$  mass hypothesis and a  $p\pi^-$  ( $\bar{p}\pi^+$ ) hypothesis. The background is dominated by combinatoric counts and the observed masses,  $496 \pm 4 \text{ MeV}/c^2$  and  $1116 \pm 7 \text{ MeV}/c^2$ , are consistent with values listed in the PDG [21] for  $K_S^0$  and  $\Lambda$  respectively. The  $K_S^0$  and  $\Lambda$  particles used in the  $v_2$  analysis are from the kinematic region of  $0.20 \leq p_t \leq 3 \text{ GeV}/c$  and  $|y| \leq 1.0$ . To compensate for limited statistics,  $\Lambda$  and  $\bar{\Lambda}$  are summed together. To reduce the combinatoric background, for  $K_S^0$ , pion-like tracks are required to have a distance of closest approach  $dca > 1.0 \text{ cm}$ , while for  $\Lambda$ , the pion-like tracks have a  $dca > 1.5 \text{ cm}$  and the proton-like

tracks have a dca  $> 0.8$  cm. Tracks are determined to be either proton-like or pion-like based on their energy loss (dE/dx) in the TPC gas. The yield from the enhancement in the invariant mass peaks in each  $\phi$ ,  $p_t$  bin is used to evaluate  $v_2 = \langle \cos(2\phi) \rangle$  as a function of  $p_t$ . This method enables us to measure identified particle flow beyond the  $p_t$  range where dE/dx particle identification fails.

The event plane, an experimental estimator of the true reaction plane [10], is calculated from the azimuthal distribution of tracks using cuts similar to those used in reference [11]. To avoid auto-correlations, only tracks excluded from the neutral vertex reconstruction are used in the event plane calculation. The observed  $v_2$  is corrected to account for the imperfect event plane resolution estimated using the method of subevents described previously [10]. The maximum resolution correction factor for the  $K_S^0$  and  $\Lambda$  analysis is found to be  $0.681 \pm 0.004$  and  $0.582 \pm 0.007$  respectively and is reached in the centrality corresponding to 25 – 35% of the measured cross section, where the relative multiplicity distribution is used to estimate the event centrality as in reference [11].

For this analysis, three sources contribute to systematic errors in the measured anisotropy parameters: (1) particle identification; (2) background subtraction; (3) non-reaction plane related correlations contributing to  $v_2$  such as resonance decays or Coulomb and Bose-Einstein correlations [22, 23]. The first two sources are estimated by examining the variation in  $v_2$  after changing several track, event and neutral vertex cuts and are found to contribute an error of less than  $\pm 0.005$  to  $v_2$ . A previous study used the correlation of event plane angles from subevents to estimate the magnitude of non-reaction plane related correlations [12]. That analysis showed that these effects which always act to increase the measured value of  $v_2$  above its true value typically contribute a systematic error to  $v_2$  of -0.005, but that the magnitude is larger in the more peripheral events where the error increases to about -0.035 for the centrality corresponding to 58 – 85% of the measured cross section.

## RESULTS

The centrality dependence of  $v_2$  as a function of transverse momentum calculated from 201 thousand minimum bias and 180 thousand central events is shown in figure 2. The two particles show a similar  $p_t$  dependence in the respective centralities with more flow in the more peripheral collisions. This is similar to observations made previously at the same energy [12] where the agreement with hydrodynamic calculations in the lower  $p_t$  region was interpreted as evidence for early local thermal equilibrium in all but the most peripheral events (45 – 85% of the measured cross section).

In figure 3 (left) we plot  $v_2(p_t)$  for  $K_S^0$  and  $\Lambda$  from minimum bias collisions with results from hydrodynamic model calculations [5] and  $v_2(p_t)$  for negatively charged particles [15]. The  $K_S^0$  results are in agreement with the  $v_2$  for  $K^\pm$  in the  $p_t$  range they share ( $300 \leq p_t \leq 700$  MeV/c) [12]. We observe that  $v_2$  for both strange particles increases as a function of  $p_t$  similar to the hydrodynamic model prediction, up to about 1.5 GeV/c. In the higher  $p_t$  region however ( $p_t \geq 2$  GeV/c), the values of  $v_2$  seem to be saturated. It has been suggested [6] that the shape and height of  $v_2$  above 2 – 3 GeV/c is related to energy loss in an early, high parton-density stage of the evolution.

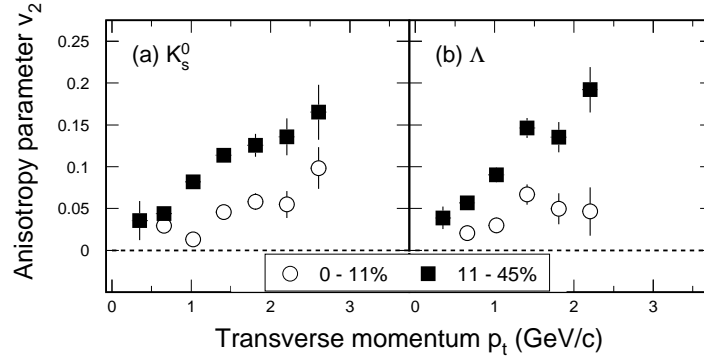


**FIGURE 2.** Elliptic flow,  $v_2(p_t)$  for  $K_S^0$  and  $\Lambda$  for central (0 – 11%) and mid-central (11 – 48%) collisions.

The  $p_t$  integrated  $v_2$  from minimum bias collisions for  $K_S^0$ ,  $\Lambda$  and negatively charged particles are shown in figure 3 (right). The integrated values of  $v_2$  are calculated by parameterizing the yield with the inverse slope parameter of exponential fits to the  $K_S^0$  or  $\Lambda$  transverse mass distributions and are dominated by the region near the particles mean  $p_t$ . The relatively larger  $v_2$  of  $\Lambda$  reflects the higher mean  $p_t$  of the  $\Lambda$  compared to the  $K_S^0$ . Hydrodynamic model calculations [5], shown as a gray-band and central line, are, within errors, in agreement with this result. The width of the gray-band indicates the uncertainty of the model calculation, mostly due to the choice of the freeze-out conditions. The increase of  $v_2$  with particle mass in figure 3 points to a significant commonality in velocities between particles of different masses that is perhaps, established early in the collision. The nature of the particles during this process however, whether parton or hadron, and the degree of thermalization remains unclear.

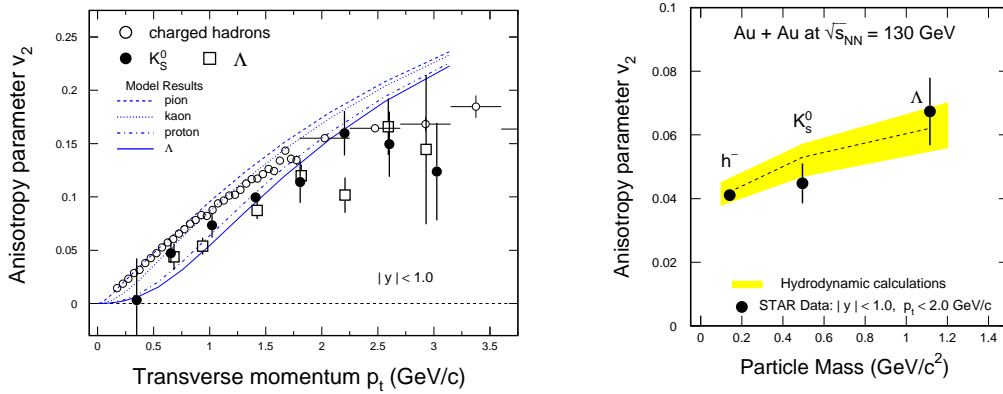


**FIGURE 3.** Elliptic flow,  $v_2$  for  $K_S^0$  and  $\Lambda$  as a function of  $p_t$  from minimum bias Au+Au collisions compared to results from hydrodynamic model calculations and  $v_2$  of negatively charged particles [15] (left). Integrated azimuthal anisotropy parameters  $v_2$  as a function of particle mass with a gray-band and central line indicating hydrodynamic model results [5] (right).

## SUMMARY

We have reported the first measurement of  $v_2$  for  $K_S^0$  and  $\Lambda$  from Au + Au collisions at  $\sqrt{s_{NN}} = 130$  GeV and the first measurement, at this energy, of  $v_2$  above  $p_t \sim 0.8$  GeV/c for any identified particle. For both particles more flow is seen in mid-central than in central collisions. The integrated values of  $v_2$  show a mass dependence consistent with the development of a common velocity, a feature of hydrodynamic models, where local thermalization is assumed. In  $v_2(p_t)$  however, we see a strong  $p_t$  dependence only up to  $p_t \sim 2.0$  GeV/c where  $v_2$  seems to saturate, suggesting that the hydrodynamic picture is incomplete for particle production above  $p_t = 1.5 - 2.0$  GeV/c.

## ACKNOWLEDGMENTS

We thank P. Huovinen for hydrodynamic model calculations and the RHIC Operations Group at Brookhaven National Laboratory for their support and for providing collisions for the experiment. This work was supported by the Division of Nuclear Physics and the Division of High Energy Physics of the Office Science of the U.S. Department of Energy, the United States National Science Foundation, the Bundesministerium für Bildung und Forschung of Germany, the Institut National de la Physique Nucleaire et de la Physique des Particules of France, the United Kingdom Engineering and Physical Sciences Research Council, and the Russian Ministry of Science and Technology.

## REFERENCES

1. Sorge, H., *Phys. Rev. Lett.*, **82**, 2048–2051 (1999).
2. Sorge, H., *Phys. Lett.*, **B82**, 251–256 (1997).
3. Ollitrault, J.-Y., *Phys. Rev.*, **D46**, 229–245 (1992).
4. Zhang, B., Gyulassy, M., and Ko, C. M., *Phys. Lett.*, **B455**, 45–48 (1999).
5. Huovinen, P., Kolb, P. F., Heinz, U. W., Ruuskanen, P., and Voloshin, S. A., *Phys. Lett.*, **B503**, 58–64 (2001).
6. Gyulassy, M., Vitev, I., and Wang, X. N., *Phys. Rev. Lett.*, **86**, 2537–2540 (2001).
7. Teaney, D., Lauret, J., and Shuryak, E. V., *Phys. Rev. Lett.*, **86**, 4783–4786 (2001).
8. Lin, Z.-w., and Ko, C. M., *Phys. Rev.*, **C65**, 034904 (2002).
9. Voloshin, S., and Zhang, Y., *Z. Phys.*, **C70**, 665–672 (1996).
10. Poskanzer, A. M., and Voloshin, S. A., *Phys. Rev.*, **C58**, 1671–1678 (1998).
11. Ackermann, K. H., et al., *Phys. Rev. Lett.*, **86**, 402–407 (2001).
12. Adler, C., et al., *Phys. Rev. Lett.*, **87**, 182301 (2001).
13. Lacey, R. A., *Nucl. Phys.*, **A698**, 559–563 (2002).
14. Park, I. C., et al., *Nucl. Phys.*, **A698**, 564–567 (2002).
15. Snellings, R. J. M., *Nucl. Phys.*, **A698**, 193–198 (2002).
16. Ackermann, K. H., et al., *Nucl. Phys.*, **A661**, 681–685 (1999).
17. Adler, C., et al., *Nucl. Instrum. Meth.*, **A461**, 337–340 (2001).
18. Wieman, H., et al., *IEEE Trans. Nucl. Sci.*, **44**, 671–678 (1997).
19. Betts, W., et al., *IEEE Trans. Nucl. Sci.*, **44**, 592–597 (1997).
20. Klein, S. R., et al., *IEEE Trans. Nucl. Sci.*, **43**, 1768–1772 (1996).
21. Groom, D. E., et al., *Eur. Phys. J.*, **C15**, 1–878 (2000).
22. Dinh, P. M., Borghini, N., and Ollitrault, J.-Y., *Phys. Lett.*, **B477**, 51–58 (2000).
23. Borghini, N., Dinh, P. M., and Ollitrault, J.-Y., *Phys. Rev.*, **C62**, 034902 (2000).